

Stability of Two-Dimensional Tessellation Ice on the Hydroxylated β -Cristobalite (100) Surface

Zhong-Yuan Lu,^{*,†} Zhao-Yan Sun,^{*,‡} Ze-Sheng Li,[†] and Li-Jia An[‡]

Institute of Theoretical Chemistry, State Key Laboratory of Theoretical and Computational Chemistry, Jilin University, 130023 Changchun, People's Republic of China, and Changchun Institute of Applied Chemistry, State Key Laboratory of Polymer Chemistry and Physics, Chinese Academy of Sciences, 130022 Changchun, People's republic of China

Received: September 21, 2004; In Final Form: December 23, 2004

Monolayer adsorbed water on the β -cristobalite (100) surface is studied via classical molecular dynamics simulations. The ordered two-dimensional (2D) tessellation ice structure (i.e., the four-membered and the eight-membered rings appear alternatively) is justified at low temperatures in the simulations. The stability of this possible new ice phase is further investigated by heating the system from 5 to 300 K. An order–disorder structural transition is observed between 100 and 200 K, featuring the melting process of the tessellation ice. This process is characterized by the water oxygen–oxygen radial distribution function, the coordination number, the distance vector between the center of mass of the oxygen and the hydrogen atoms in water, the mean square displacement of oxygen in water, and the vibrational density of state. The above techniques show consistency on that the order–disorder transition temperature of the 2D tessellation ice is far below 300 K. The 2D tessellation ice structure is also obtained via density functional calculations with different generalized gradient approximations. By comparing the calculated adsorption and the lateral energies between different methods, we find that the melting temperature of the specific 2D ice structure is strongly method dependent. Therefore, further experimental works are urged to justify this possible new ice phase and probe its stability.

1. Introduction

Water, the most common and abnormal liquid, has intrigued a lot of researchers owing to its unique properties directly related to the life systems and environment. For example, most of the biological processes can only be possible in water and different patterns of water circles exactly control the weather in the globe. Plenty of works have been done for a better understanding of the structural and dynamic properties of water.¹ However, due to the complexity of the hydrogen bond network, many questions still remain. Only recently improvements had been made to correctly extract the oxygen–oxygen pair distribution function from scattering experiments.² In the theoretical part, about 50 water models have been proposed, trying to elucidate the water structural and thermodynamic properties in a consistent way.³

As a powerful tool, the molecular dynamics (MD) simulation technique has been successfully applied on, for example, predicting the water structure on surfaces, either from the first principles or via classical pairwise interaction potentials.^{4–7} Although the *ab initio* MD (AIMD),⁸ treating the electrons explicitly with density functional theory (DFT) and the force acting on the nuclear due to electrons on the fly, is genuinely predictive, the classical force field method still serves as a demanding tool for accessing much longer time scales and for larger systems.⁹ Of course, in the spirit of multiscale simulation, one may need to combine the virtue of both AIMD and classical

MD methods for obtaining a clear overview of the water properties.

Very recently, AIMD simulations on bulk water were re-evaluated by Grossman et al., who had found too low water diffusivity and a clear over-structuring compared to experiments, despite the successfulness of the method.¹⁰ Moreover, due to the small size of the simulation cell in a typical AIMD, the possible ordered water structure might be artificially imposed by the simulation box. Indeed, also in classical MD, limited system size does underestimate the diffusivity and over-structure the liquid. However, one can easily increase the system size in a classical MD to relieve this problem, with the computational cost increasing at most with N^2 , where N is the number of particles. On the contrary, the computational cost goes up with N^3 , where N is the number of basic functions per atom in AIMD.

Recently, a 2D tessellation water structure, that is, a quadrangular and octagonal patterned hydrogen bond network, was proposed based on an AIMD simulation.¹¹ The result is nontrivial because it predicts a possible new ice phase when water molecules are adsorbed on the hydroxylated β -cristobalite (100) surface. As the (100) and the (111) surfaces of β -cristobalite are rationalized to be the prototype of the surface of amorphous silica,¹² this 2D tessellation ice structure may widely exist in many technological applications. The structure was reported to be even stable until 300 K in the 4-ps AIMD simulation.¹¹ However, only a (1×1) surface cell was adopted; therefore, this ordered water structure might be stabilized by the periodic boundary condition during the MD simulation. In fact, the quadrangular water pattern was reported to be popular in small water clusters¹³ and also was suggested experimentally to appear inside a nanotube forming an octagonal section water

* To whom correspondence should be addressed. E-mail: luzhy@mail.jlu.edu.cn (Z.-Y.L.); zysun@ns.ciac.jl.cn (Z.-Y.S.). Phone: 0086 431 8498017 (Z.-Y.L.); 0086 431 5262137 (Z.-Y.S.). Fax: 0086 431 8945942 (Z.-Y.L.); 0086 431 5262126 (Z.-Y.S.).

[†] Jilin University.

[‡] Chinese Academy of Sciences.

pipe.¹⁴ In the latter case, the water structure undergoes a continuous solid-to-liquid transition far below room temperature. Furthermore, a high-density liquid water phase was recently observed in the interface of ice and amorphous SiO_2 (rehydroxylated) below the melting temperature of bulk ice, emphasizing the strong hydrogen bond induction effect of the surface on water.¹⁵ We also notice that only physical adsorption takes place on the hydroxylated silica surface, and the hydrogen bonds in the two-dimensional (2D) tessellation ice are not so strong compared to those in bulk ice;¹¹ thus, the conclusion of Yang et al. showing that the structure is even stable until 300 K may need further justification. Therefore, combining the above facts, we argue that the 2D tessellation ice structure may not be so stable as shown in the AIMD simulation, and the motivation of the present research is to study the stability of the proposed 2D tessellation ice in detail.

Simulations of water adsorption on silica surfaces were carried out in different respects. Lee and Rossky had systematically studied the structural and dynamic properties of water between two hydrophobic or hydrophilic silica surfaces.¹⁶ Warne et al. studied the effects of increasing the ionic strength of water, which was confined between two amorphous silica surfaces.¹⁷ Puibasset and Pellenq applied the grand canonical Monte Carlo method to study the water structure on hydrophilic mesoporous and plane silica substrates.¹⁸ The natural way to study the stability of the 2D tessellation ice absorbed on the hydroxylated β -cristobalite (100) surface should be applying the same simulation method as in ref 11 but increasing the box length to minimize the effects of the small system size. However, it is very difficult to enlarge the system size in a typical AIMD simulation due to the computation cost. We notice that, recently, classical MD simulation methods were successfully applied to study the adsorption of water molecules on the surface of, for example, MgO .^{19,20} Thus, in this research, we adopt classical MD to simulate a larger β -cristobalite surface system and try to study the stability of the corresponding 2D tessellation ice. In this paper water molecules are modeled flexible to partially account for the polarizability, and a class II force field, COMPASS,²¹ which is originated from accurate ab initio calculations, is used. The force field was optimized for the simulations of condensed phases.²¹ The melting process of the 2D tessellation ice is characterized by calculating the O–O radial distribution function, the coordination number of oxygen, the distance vector between the center of mass of the oxygen and the hydrogen atoms in water, the mean square displacement (MSD) of oxygen in water molecules, and the vibrational density of state (VDOS). The above techniques show consistency on that the order–disorder transition temperature of the 2D tessellation ice is far below 300 K, in contrast to the prediction in ref 11. The 2D tessellation ice structure is also obtained via density functional calculations with PW91²² and rPBE²³ generalized gradient approximations. By comparing the adsorption and the lateral energies obtained from the above three methods, we find that the melting temperature of this specific 2D ice structure is sensitive to the calculation method selection. Such an interesting result urges experimental works to verify the 2D tessellation ice structure and elucidates its stability by heating.

2. Model and Simulation Details

In this study, the water molecule is modeled flexible, and the interaction parameters are taken from the COMPASS force field.²¹ The (100) surface of β -cristobalite, modeled by a slab geometry with three-dimensional periodic boundary conditions, is cut from the crystal 11 atomic layers thick.²⁴ The slabs are

separated by 50 Å of vacuum, which is large enough to ignore the interaction between the adjacent slabs in the Z direction. The dangling bonds on the top and bottom surfaces are saturated by hydrogen atoms; therefore, the top surface is changed to be hydroxylated.

The well-known water models such as SPC/E^{25,26} and TIP3P²⁷ are not used, because bulk water modeled at ambient conditions via the COMPASS force field can give comparable results. Most importantly, both water and the surface atom interaction parameters in the COMPASS force field are obtained in a consistent manner to fit the need of condensed matter simulations (details on the COMPASS force field could be found in ref 21). It should be noted that a recently proposed AMOEBA water model²⁸ may be more accurate for water simulations because the AMOEBA water is modeled flexible and polarizable.

For further testing the applicability of the COMPASS force field, we carry out the MD simulations on crystal β -cristobalite at ambient conditions. The crystal is first generated with $Fd3m$ space group and then by breaking the symmetry and modeled allowing all atoms movable. The eight unit cells are used, containing 192 atoms. The Ewald summation method is applied on both van der Waals and electrostatic interaction calculations. After an 80-ps simulation we then minimize the energy and measure the structure parameters in the model. The calculated values are 7.142 Å (lattice constant), 1.611 Å (Si–O bond length), 107.5 and 110.0° ($\angle\text{O–Si–O}$ angle), and 148.4 and 150.1° ($\angle\text{Si–O–Si}$ angle), which are in good agreement with the experimental values 7.16 Å, 1.611 Å, 107.8°, 112.8°, and 146.7°.²⁹

We add four water molecules, which correspond to monolayer adsorption,¹¹ with different adsorption arrangements in a (1 × 1) surface unit cell. Then the cell is copied in the X and Y directions to form a 16 times larger superlattice. The energy of the structure is minimized with the BFGS algorithm.³⁰ All possible adsorption configurations are compared in energy, and the 2D tessellation ice is found to be the most stable structure. The adsorption energy per molecule of the tessellation ice is 47 kJ/mol, which is smaller than the value (69 kJ/mol) in the density functional calculations.¹¹ However, 47 kJ/mol is comparable to the estimated adsorption energy of water on the surfaces of metals,³¹ where icelike structures have been identified at low temperatures in an ultrahigh vacuum. This value corresponds to roughly two to three hydrogen bonds per molecule.⁶ The adsorption energy difference between our molecular mechanics (MM) and ab initio calculations is of key importance to the stability of the 2D tessellation ice. We will discuss this in detail in section 3.

Figure 1 shows the optimized geometry of 2D tessellation ice obtained via MM minimization. For clarity, the surface atoms are omitted. All water molecules are basically coplanar covering the surface. The 2D water network is composed of four-membered and distorted eight-membered water rings alternatively. Each water molecule is saturated with hydrogen bonds: three to nearby water molecules and one to the surface hydroxyl group. The measured O–O distance shows that the H bonds are not equal. The lengths of the side of the four-membered ring range from 2.90 to 2.94 Å, whereas the O–O lengths connecting the adjacent four-membered rings are 2.88, 2.92, and 3.31 Å. These values are larger than the O–O distance in ice-Ih, which is 2.76 Å,³² indicating weaker H bonds in the 2D tessellation ice. The large value (3.31 Å) shows very weak H bonding in the octagonal water ring. Therefore, by heating the

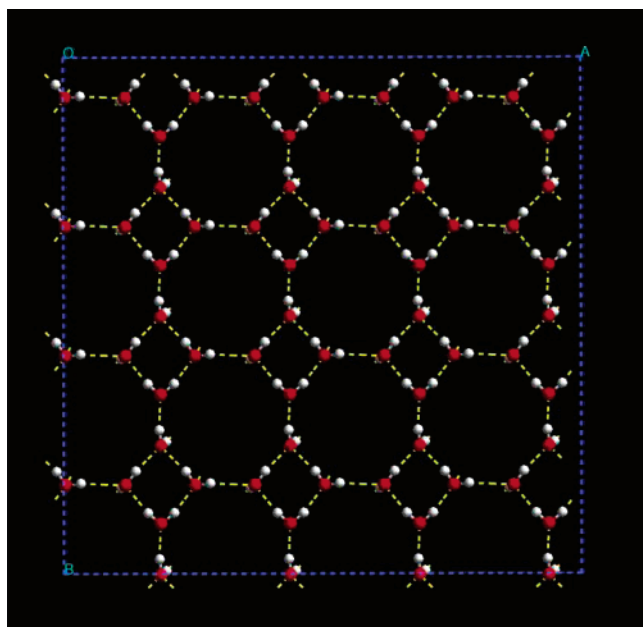


Figure 1. Optimized geometry of 2D tessellation ice.

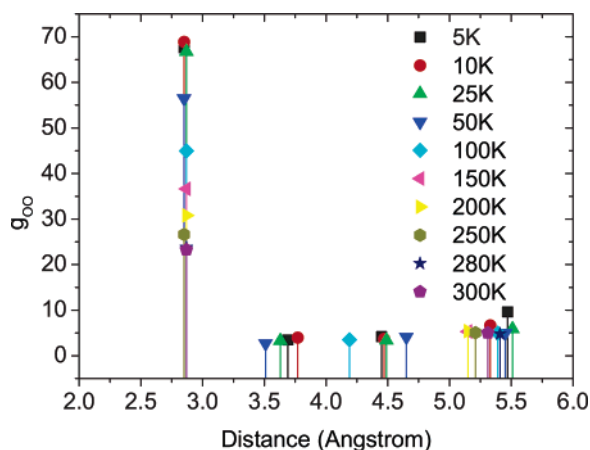


Figure 2. Peak positions and heights of the calculated radial distribution functions, g_{OO} , at different temperatures.

system, a structural transition may take place accompanied with weak H bonds breaking at a temperature below the melting point of ice-Ih.

Starting from the optimized geometry of the 2D tessellation ice including the surface atoms, a series of MD simulations are carried out at different temperatures. The total volume and the number of the particles are kept constant during the simulations. The temperature is controlled constant via the Nosé–Hoover method.³³ For calculating the van der Waals interactions, a spherical cutoff method with radius 12.0 Å is adopted.³⁴ The Ewald summation method is applied to accurately calculate long-range electrostatic interactions, which is important in the water simulations.³⁵ A typical simulation is 200-ps long, with a small integration time step of 0.4 fs for properly taking into account the fast movement of hydrogen atoms.

3. Results and Discussion

Figure 2 shows the peak positions and heights of the calculated O–O radial distribution functions, g_{OO} , at different temperatures. At low temperatures such as 5, 10, and 25 K, g_{OO} shows four peaks below 6 Å, and the peak positions and heights at these three temperatures change only a little. This means that the 2D tessellation ice is stable at very low

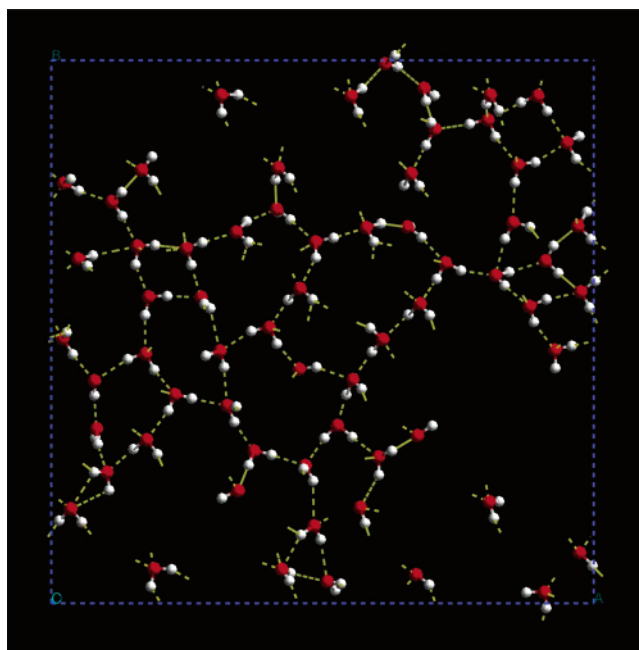


Figure 3. Snapshot of the surface adsorbed water molecules after 200 ps of simulation at 150 K.

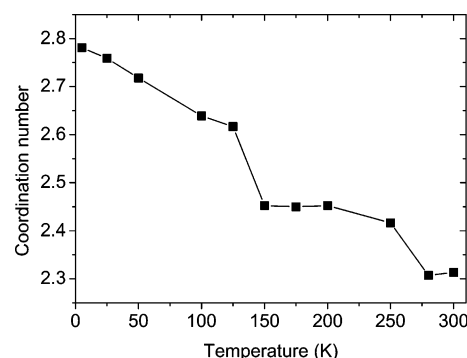


Figure 4. Calculated coordination numbers of water molecules at different temperatures. The first minimum of g_{OO} is taken as 3.3 Å, in accord with Figure 3B in ref 36.

temperatures. Increasing the temperature to 50 K, there are still four peaks in g_{OO} , but the peak positions and heights show larger variance compared to the low-temperature cases. The four peaks below 6 Å indicate a regular lattice pattern. Therefore, we conclude that at lower temperatures this pattern does not change much, whereas at 50 K the pattern is distorted. While increasing the temperature to 100 K, only three peaks are left in the g_{OO} curve. This implies that the regular tessellation pattern is partially broken when heating. Increasing the temperature to 150 K induces another structure transition; only two peaks appear in g_{OO} . Further heating the system until 300 K does not change the peak positions and heights much. As reported by Puibasset and Pellenq,¹⁸ this two-peak nature in g_{OO} (one at 2.85 and another around 5.0 Å) is characteristic of the bi-dimensional structure of water. Therefore, by increasing the temperature, we can observe two structural transitions locating at 100 and 150 K, respectively. The first transition shows the local breaking of the regular 2D tessellation pattern, and the second one corresponds to the transition from 2D ice to 2D water. Figure 3 shows the snapshot of the surface-adsorbed water molecules after a 200-ps simulation at 150 K. Apparently the ordered tessellation structure does not exist anymore.

Figure 4 shows the calculated coordination number (N_c) of the water molecules at different temperatures. N_c is defined as

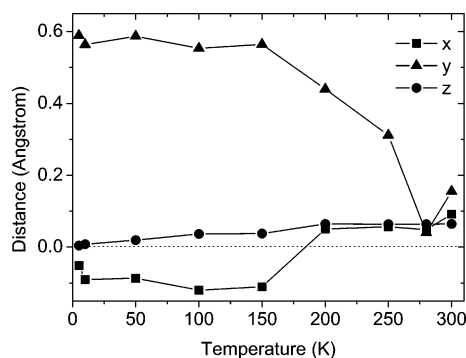


Figure 5. Distance between the center of mass of oxygen and hydrogen atoms in water at different temperatures.

$N_c = 4\pi\rho\int_0^{r_{\min}} r^2 dr g_{OO}(r)$, where ρ is the number density of water and r_{\min} is the location of the first minimum in g_{OO} . This definition does not take into account the angular dependence of H bonding. Although recently Wernet et al. have proposed a parabola-like H bonding boundary line, which depends both on distance and on the angle between two nearest-neighbor H bond acceptor molecules,³⁶ we still adopt the coordination number definition shown above due to its extensive usage. In the temperature region between 5 and 125 K, N_c decreases from 2.78 to 2.62 roughly linearly. Then there is an apparent drop of N_c when heating the system from 125 to 150 K. Further heating until 250 K, N_c does not change much. However, N_c decreases drastically again with temperature increasing to 280 K. For bulk water at ambient conditions, N_c is estimated experimentally to be 4.7 (ref 2) which is larger than our calculated values. It should be noted that for the water adsorbed between two hydrophilic silica walls, Lee and Rossky obtained a similar coordination number $N_c = 2.6$ (ref 16) for the water molecules. Our maximum N_c is 2.78, showing the nature of planar three coordination of water molecules in a four-membered or eight-membered ring. Moreover, the first drop on N_c indicates the breaking of the 2D tessellation H bond pattern at around 150 K, which is in agreement with our discussion on the g_{OO} . From 150 to 250 K, N_c basically keeps constant, which corresponds to the strong monolayer adsorption of water molecules on the surface. The second drop on N_c may be attributed to the constant number of water molecules in the simulations. By heating, some of the water molecules aggregate locally, leaving the rest of the water molecules adsorbed onto the surface without neighbors. Therefore, we may observe a drastic decrease on the coordination number.

The ordered water molecules possess periodical structure; thus, the distance vector between the center of mass of the oxygen and the hydrogen atoms in water may show anisotropic orientation preference. Thus, the three Cartesian components of the total vector between the centers L_x , L_y , and L_z are shown in Figure 5 at different temperatures. Despite small drops on L_x and L_y at very low temperatures, the three components are basically constant below 150 K. This partially indicates the stability of the 2D tessellation ice structure at low temperatures. While heating to 200 K, all three components change drastically toward 0. Further heating does not change L_x and L_z much but will reduce L_y a lot. Above 280 K, all three values increase with strong fluctuations. We may assign 150 K as a transition temperature, before which the 2D tessellation structure is (partially) stable and afterward the 2D ice melts into 2D strong adsorbed liquid water. Furthermore, L_x , L_y , and L_z are anisotropic at low temperatures, whereas at high temperatures the anisotropy disappears. This may relate to the order-disorder transition in our system.

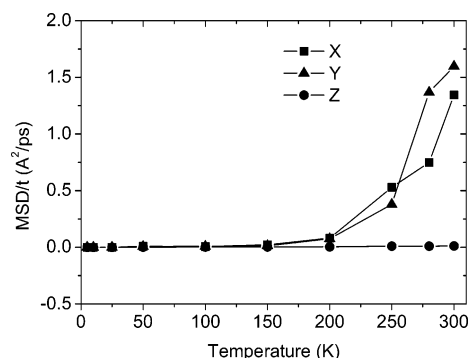


Figure 6. Time-averaged MSD of oxygen in 2D water at different temperatures.

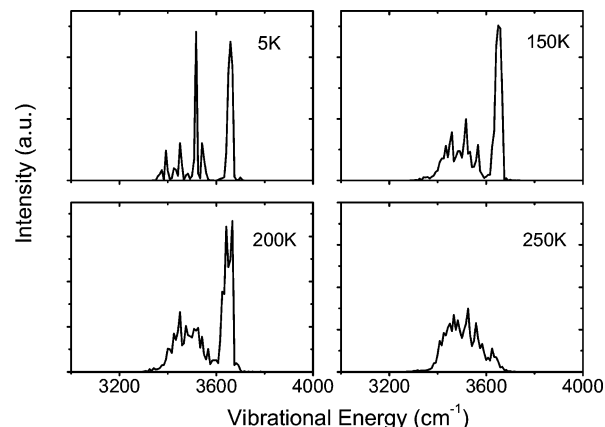


Figure 7. VDOS of 2D water at different temperatures.

The 2D water dynamics during heating may be reflected by the MSD. Via the Einstein relation, time-averaged MSD gives the self-diffusion coefficient D . Figure 6 shows the three Cartesian components of the time-averaged MSD of oxygen in water at different temperatures. Below 150 K, the values of all three components are very small, and there is no strong anisotropy between them. This indicates that the water molecules only move around at the equilibrium positions at low temperatures. Above 150 K, D_x and D_y increase drastically with increasing temperature, whereas D_z changes only a little. This manifests that the movement of water molecules in the Z direction is highly restricted due to the strong adsorption on the hydrophilic surface. Furthermore, D_x and D_y are roughly two orders larger than D_z at 300 K. The strong anisotropy was also observed in the recent simulations on the surface melting of ice-1h.³⁷ In their cases D_z is larger than the other components. In our case the dynamics of water is controlled mainly by the strong adsorption on the hydrophilic surface; therefore, we can observe special Z direction anisotropy.

The VDOS can be obtained from the Fourier transform of the short time velocity autocorrelation function:

$$\text{VDOS}(\omega) = \int_0^\infty \exp(-i\omega t) \langle \vec{v}(t) \cdot \vec{v}(0) \rangle dt \quad (1)$$

Here, $\vec{v}(t)$ is the velocity of one atom at time t and ω is the vibrational energy.³⁴ VDOS manifests the difference of the dynamics of water in distinct environments. Figure 7 shows the calculated VDOS of adsorbed water at different temperatures. The peaks located at the right side of 3000 cm^{-1} are OH stretching modes, which are sensitive to the variation of the H bonding environment. Therefore, in Figure 7 only the parts of the VDOS with wavenumber larger than 3000 cm^{-1} are shown. At 5 K, there are apparently five peaks located at 3658, 3541,

3516, 3450, and 3392 cm^{-1} , respectively. In this bond stretching part of VDOS, the smaller wavenumber corresponds to stronger H bonding. Therefore, the peak at 3658 cm^{-1} relates to the weak H bond connecting the ice quadrangles with O—O distance equal to 3.31 Å. The peak at 3392 cm^{-1} corresponds to the strong H bonding between water and the surface hydroxyl groups, with the O—O distance 2.65 Å. The other three peaks can be specified relating to the H bonding inside the four-membered ring, the H bond connecting the quadrangles, and the in-surface H bond between the adjacent germinal surface hydroxyl groups. By heating to 150 K, which is assigned to be the order—disorder transition temperature, the five-peak nature does not change. However, instead of distinct sharpness of the peak, there is apparent overlapping between the first four peaks. Until 200 K, the peak with the highest wavenumber still exists, but the first four peaks cannot be easily identified due to strong overlapping. With further heating to 250 K, the sharp peak corresponding to the weakest H bond totally disappears, and we observe a broad band of VDOS with a value larger than 3000 cm^{-1} . The vanishing of the peak located at 3658 cm^{-1} may relate to the structure transition from 2D ice to 2D water. Therefore, from the discussion of VDOS, we conclude that the order—disorder transition temperature of the 2D tessellation ice may be above 200 K.

Our calculations shown above suggest that the order—disorder structural transition of 2D tessellation ice may occur between 150 and 200 K, far below the predicted 300 K in a recent AIMD simulation.¹¹ However, the adsorption energy difference between our classical MM result and the ab initio value from ref 11 (around 30% difference) is of the key importance to the stability of the 2D tessellation ice. To understand the energy difference, we first redo the minimization process as in ref 11 by using CASTEP³⁸ and try to reproduce their results. Thus, we follow all the details; that is, the generalized gradient approximation PW91²² is used for the exchange correlation energy; electron—core interactions are described by the Vanderbilt ultrasoft pseudopotential;³⁹ and the Monkhorst—Pack scheme⁴⁰ with $2 \times 2 \times 1$ k points is used to integrate in the surface Brillouin zone. However, the Kohn—Sham orbital is expanded in plane waves up to a kinetic energy cutoff of 300 eV (which is 350 eV in ref 11). We have adopted 300 eV because Yang et al. also take this value in their AIMD simulations.¹¹ Moreover, the geometry optimization criterion is set to be 2×10^5 eV per atom instead of 1×10^4 eV per atom used by Yang et al. We obtain the 2D tessellation ice structure. The adsorption energy is also reproduced to be 71.8 kJ/mol. However, the equilibrium geometry parameters are somewhat different from the results of ref 11. We notice that PW91 functionals are recently less approved to be accurate enough for liquid water calculations compared to rPBE functionals.^{9,41} Therefore, we adopt rPBE²³ instead of PW91 in the minimization process again while keeping all other control factors unchanged. We also obtain the 2D tessellation ice structure. However, the adsorption energy is 48.7 kJ/mol, which is very similar to our classical MM value (46.9 kJ/mol). Such an interesting result is nontrivial because it raises the question which method is suitable to discuss the stability of the 2D tessellation ice and urges experimental works to elucidate it. The large energy difference between the PW91/rPBE functionals also highlights the conundrum in AIMD of which functional should be suitable in a specific simulation of water. Moreover, it should be mentioned that Perdew et al. have noted that rPBE weakens the intramolecular bonds in an isolated water, although it describes liquid water better.⁴²

TABLE 1: Calculated Adsorption and Lateral Energies from Three Different Methods^a

	adsorption energy (kJ/mol)	lateral energy (kJ/mol)
PW91	71.8	35.0
rPBE	48.7	22.0
MM	46.9	30.1
ref 11	69.0	41.2

^a The values from ref 11 are also based on the PW91-GGA approximation of DFT calculations.

The competition between lateral and water—surface interactions is also of importance to the stability of the 2D tessellation ice. We have obtained these energy values from PW91, rPBE, and classical MM methods and listed them in Table 1. The adsorption energy itself manifests the stability of the 2D tessellation ice structure. From Table 1 we can find that the 2D ice structures in the MM and rPBE cases are less stable compared to the PW91 case due to their smaller adsorption energies. The values (47–49 kJ/mol) are also comparable to that obtained for water overlayer adsorption on the MgO surface which is 43.8 kJ/mol (see Table 2 of ref 20). With such an adsorption energy, the 2D periodical water structure cannot exist at 300 K.²⁰ The lateral energy corresponds to the stability of the stand-alone 2D ice structure. By heating, the water molecules easily break their mutual ordered connection in the case of rPBE due to the small lateral energy. The difference between the adsorption energy and the lateral energy gives the water—surface interaction, which is the weakest in the case of MM and strongest in the case of PW91. Comparing the lateral water—water interactions and the water—surface interactions in the three cases, we find that, by heating, the MM resulting in a 2D ice structure will melt in a different way than that from rPBE, although in these two cases we obtain similar adsorption energies. The structure from PW91 is the most stable one. The above results at least show that the melting temperature of the 2D tessellation ice structure is strongly method-dependent. These provide further motivations for experimentally probing the stability of this possible new ice phase which has not been performed so far.

4. Conclusion

In this paper, the ordered 2D tessellation ice structure, when water molecules are adsorbed on a (100) β -cristobalite surface, is justified at low temperatures via classical MD simulations. The structure is partially stable until 150 K in the simulations, in contrast to the predicted 300 K in ref 11. The stability of this new possible ice phase is characterized by the water O—O radial distribution function, the coordination number, the distance vector between the center of mass of the oxygen and the hydrogen atoms in water, the mean square displacement of oxygen in water, and the VDOS. All the above techniques show consistency in that the order—disorder transition temperature of the 2D tessellation ice should be far below 300 K. The 2D tessellation ice structures are also obtained via density functional calculations. We compare the adsorption and the lateral energies obtained from the three methods and find that the melting temperature of this specific 2D ice structure is strongly method-dependent. Thus, further experimental works are indeed needed to justify this possible new ice phase and investigate its stability.

Acknowledgment. This work is supported by the National Science Foundation of China (20304015, 20490220, 20404005).

References and Notes

- (1) *Water, a Comprehensive Treatise*; Franks, F., Ed.; Plenum Press: New York, 1972; Vol. 1.

- (2) Head-Gordon, T.; Hura, G. *Chem. Rev.* **2002**, *102*, 2651.
- (3) Guillot, B. *J. Mol. Liq.* **2002**, *101*, 219.
- (4) Kuo, I.-F. W.; Mundy, C. J. *Science* **2004**, *303*, 658.
- (5) Lilach, Y.; Buch, V.; Asscher, M. *J. Chem. Phys.* **2003**, *119*, 11899.
- (6) Odelius, M.; Bernasconi, M.; Parrinello, M. *Phys. Rev. Lett.* **1997**, *78*, 2855.
- (7) Robinson, G. W.; Zhu, S.-B.; Singh, S.; Evans, M. W. *Water in Biology, Chemistry and Physics: Experimental Overviews and Computational Methodologies*; World Scientific: New York, 1996.
- (8) Car, R.; Parrinello, M. *Phys. Rev. Lett.* **1985**, *55*, 2471.
- (9) Fernandez-Serra, M. V.; Artacho, E. arXiv:cond-mat/0407237, 2004.
- (10) Grossman, J. C.; Schwegler, E.; Draeger, E. W.; Gygi, F.; Galli, G. *J. Chem. Phys.* **2004**, *120*, 300.
- (11) Yang, J.; Meng, S.; Xu, L. F.; Wang, E. G. *Phys. Rev. Lett.* **2004**, *92*, 146102.
- (12) Chuang, I.-S.; Maciel, G. E. *J. Phys. Chem. B* **1997**, *101*, 3052.
- (13) Kabrede, H.; Hentschke, R. *J. Phys. Chem. B* **2003**, *107*, 3914.
- (14) Kolensnikov, A. I.; Zanotti, J.-M.; Loong, C.-K.; Thiagarajan, P.; Moravsky, A. P.; Loutfy, R. O.; Burnham, C. J. *Phys. Rev. Lett.* **2004**, *93*, 035503.
- (15) Engemann, S.; Reichert, H.; Dosch, H.; Bilgram, J.; Honkimaki, V.; Snigirev, A. *Phys. Rev. Lett.* **2004**, *92*, 205701.
- (16) Lee, S. H.; Rossky, J. P. *J. Chem. Phys.* **1994**, *100*, 3334.
- (17) Warne, M. R.; Allan, N. L.; Cosgrove, T. *Phys. Chem. Chem. Phys.* **2000**, *2*, 3663.
- (18) Puibasset, J.; Pellenq, R. J.-M. *J. Chem. Phys.* **2003**, *119*, 9226.
- (19) Girardet, C.; Hoang, P. N. M.; Marmier, A.; Picaud, S. *Phys. Rev. B* **1998**, *57*, 11931.
- (20) Marmier, A.; Hoang, P. N. M.; Picaud, S.; Girardet, G.; Lynden-Bell, R. M.; *J. Chem. Phys.* **1998**, *109*, 3245.
- (21) Sun, H. *J. Phys. Chem. B* **1998**, *102*, 7338.
- (22) Wang, Y.; Perdew, J. P. *Phys. Rev. B* **1991**, *44*, 13298.
- (23) Zhang, Y.; Yang, W. *Phys. Rev. Lett.* **1998**, *80*, 890.
- (24) Iarlari, S.; Ceresoli, D.; Bernasconi, M.; Donadio, D.; Parrinello, M. *J. Phys. Chem. B* **2001**, *105*, 8007.
- (25) Berendsen, H. J. C.; Grigera, J. R.; Straatsma, T. P. *J. Phys. Chem.* **1987**, *91*, 6269.
- (26) Kusalik, P. G.; Svishchev, I. M. *Science* **1994**, *265*, 1219.
- (27) Jorgensen, W. L.; Chandrasekhar, J.; Madura, J. D.; Impey, R. W.; Klein, M. L. *J. Chem. Phys.* **1983**, *79*, 926.
- (28) Ren, P.; Ponder, J. W. *J. Phys. Chem. B* **2003**, *107*, 5933.
- (29) Wright, A. F.; Leadbetter, A. J. *Philos. Mag.* **1975**, *31*, 1391.
- (30) Press, W. H.; Teukolsky, S. A.; Vetterling, W. T.; Flannery, B. P. *Numerical Recipes in FORTRAN: The Art of Scientific Computing*; Cambridge University: Cambridge, 1992.
- (31) Thiel, P. A.; Madey, T. E. *Surf. Sci. Rep.* **1987**, *7*, 211.
- (32) *The structure and properties of water*; Eisenberg, D., Kauzmann, W., Eds.; Oxford University, New York, 1969.
- (33) Hoover, W. G. *Phys. Rev. A* **1985**, *31*, 1695.
- (34) Allen, M. P.; Tildesley, D. J. *Computer Simulations of Liquids*; Oxford Science: Oxford, 1987.
- (35) Ewald, P. *Ann. Phys.* **1921**, *64*, 253.
- (36) Wernet, Ph.; Nordlund, D.; Bergmann, U.; Cavalleri, M.; Odelius, M.; Ogasawara, H.; Naslund, L. A.; Hirsch, T. K.; Ojamae, L.; Glatzel, P.; Pettersson, L. G. M.; Nilsson, A. *Science* **2004**, *304*, 995.
- (37) Ikeda-Fukazawa, T.; Kawamura, K. *J. Chem. Phys.* **2004**, *120*, 1395.
- (38) Segall, M. D.; Lindan, P. L. D.; Probert, M. J.; Pickard, C. J.; Hasnip, P. J.; Clark, S. J.; Payne, M. C. *J. Phys.: Condens. Matter* **2002**, *14*, 2717.
- (39) Vanderbilt, D. *Phys. Rev. B* **1990**, *41*, 7892.
- (40) Monkhorst, H. J.; Pack, J. D. *Phys. Rev. B* **1976**, *13*, 5188.
- (41) Asthagiri, D.; Pratt, L. R.; Kress, J. D. *Phys. Rev. E* **2003**, *68*, 041505.
- (42) Perdew, J. P.; Burke, K.; Ernzerhof, M. *Phys. Rev. Lett.* **1998**, *80*, 891.